

# Evaluation of energies of isomeric SO<sub>2</sub> complexes<sup>†</sup>

Alexei V. Marchenko, Andrei N. Vedernikov, John C. Huffman and Kenneth G. Caulton\*

Department of Chemistry, Indiana University, Bloomington, IN 47405, USA.

E-mail: caulton@indiana.edu

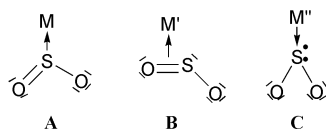
Received (in New Haven, CT, USA) 2nd December 2002, Accepted 16th December 2002

First published as an Advance Article on the web 26th February 2003

SO<sub>2</sub> binds to MHCl(CO)L<sub>2</sub> (M = Ru, Os; L = P<sup>i</sup>Pr<sub>3</sub>) to give a product in which SO<sub>2</sub> binds trans to hydride, and with an η<sup>1</sup>-SO<sub>2</sub> binding mode, planar around sulfur, as shown in part by an X-ray diffraction study for M = Ru. We have investigated the structures and energies of various isomers and insertion (of SO<sub>2</sub> into the Ru–H bond) products of the observed product to evaluate, in a fixed molecular environment, their stabilities relative to the observed product, in which SO<sub>2</sub> functions as a Lewis base. In contrast to CH<sub>2</sub> insertion into the analogous Os–H bond, insertion of SO<sub>2</sub> into Ru–H here is not strongly favored. A search of the potential energy surface shows that η<sup>1</sup>-SO<sub>2</sub> with pyramidal sulfur is not a stationary state.

## Introduction

The molecule SO<sub>2</sub> shows great versatility in interacting with metal complexes, functioning as a Lewis base in two structural modes (A and B), and also as a Lewis acid (C), in a structure distinguished from A by being pyramidal, not planar, at sulfur.<sup>1–6</sup> In such a situation, the possibility of isomerization from one binding form to another is of interest. There is a report<sup>7</sup> of a photochemical isomerization of A to B in [Ru(NH<sub>3</sub>)<sub>4</sub>Cl(SO<sub>2</sub>)]Cl, which has been further explored by diffraction methods.<sup>8</sup> There is also a report<sup>3</sup> of a thermal isomerization between A and B in Mo(CO)<sub>2</sub>(PPh<sub>3</sub>)<sub>2</sub>(SO<sub>2</sub>)(isonitrile) in the solid, with a small energy difference between them, but this could not be verified by NMR spectral data in solution. Finally, there is evidence that isomerization from A to C, because it opens up an empty metal orbital, is responsible for associative kinetics of ligand substitution in several SO<sub>2</sub> complexes of molybdenum.<sup>2,9</sup>



A key question in this field is the magnitude of the energy differences between the various M/SO<sub>2</sub> bonding forms. We report here both experimental and density functional theory (DFT) studies of precisely this question, to provide some initial orientation on when isomerization might be thermally accessible and when the higher energy of photolysis might be required.

## Results

### Reactivity of 5-coordinate d<sup>6</sup> monohydrides towards SO<sub>2</sub>

Both RuHCl(CO)(P<sup>i</sup>Pr<sub>3</sub>)<sub>2</sub> and OsHCl(CO)(P<sup>i</sup>Pr<sub>3</sub>)<sub>2</sub> readily react with SO<sub>2</sub> in both the solid state (complete conversion to the product occurs within 12 h) and in benzene solution to give products as pale yellow solids. These were characterized as RuHCl(CO)(SO<sub>2</sub>)(P<sup>i</sup>Pr<sub>3</sub>)<sub>2</sub> and OsHCl(CO)(SO<sub>2</sub>)(P<sup>i</sup>Pr<sub>3</sub>)<sub>2</sub> by

NMR and IR spectroscopy. Both show a downfield metal hydride chemical shift in <sup>1</sup>H NMR (–6.48 and –7.10 ppm, respectively) compared to their five-coordinate precursors, indicative of a ligand being present trans to the hydride. In addition, RuHCl(CO)(SO<sub>2</sub>)(P<sup>i</sup>Pr<sub>3</sub>)<sub>2</sub> was structurally characterized by X-ray diffraction (Fig. 1).

In addition to a weak Ru–H band at 2036 cm<sup>–1</sup>, the IR spectrum of RuHCl(CO)(SO<sub>2</sub>)(P<sup>i</sup>Pr<sub>3</sub>)<sub>2</sub> shows symmetric and asymmetric SO<sub>2</sub> stretching modes at 1111 and 1288 cm<sup>–1</sup>, respectively. These values are within the typical range for the η<sup>1</sup>-planar SO<sub>2</sub> complexes<sup>5,10</sup> {for example, the reported ν<sub>asym</sub>(SO) and ν<sub>sym</sub>(SO) for [Ru(NH<sub>3</sub>)<sub>4</sub>(SO<sub>2</sub>Cl)]Cl<sup>11</sup> are at 1301, 1278, 1100 cm<sup>–1</sup>} and very close to the IR data (1284 and 1109 cm<sup>–1</sup>) for the only previously characterized osmium complex containing hydride and SO<sub>2</sub>: OsHCl(CO)(SO<sub>2</sub>)(PCy<sub>3</sub>)<sub>2</sub>.<sup>12</sup> The carbonyl stretching frequency of RuHCl(CO)(SO<sub>2</sub>)(P<sup>i</sup>Pr<sub>3</sub>)<sub>2</sub> is 1965 cm<sup>–1</sup>. This high value [ν(CO) for the starting material RuHCl(CO)(P<sup>i</sup>Pr<sub>3</sub>)<sub>2</sub> is at 1910 cm<sup>–1</sup>], also found for OsHCl(CO)(SO<sub>2</sub>)(PCy<sub>3</sub>)<sub>2</sub> (1950 cm<sup>–1</sup>), indicates that the SO<sub>2</sub> ligand oxidizes the Ru center and that its Lewis acidity is comparable to that of CO [one ν(CO) stretch in RuHCl(CO)<sub>2</sub>(P<sup>i</sup>Pr<sub>3</sub>)<sub>2</sub> is at 1970 cm<sup>–1</sup>].

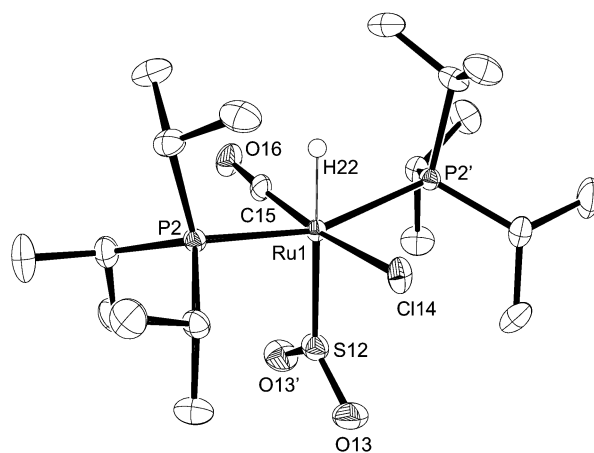


Fig. 1 ORTEP drawing (50% probability) of RuHCl(CO)(SO<sub>2</sub>)(P<sup>i</sup>Pr<sub>3</sub>)<sub>2</sub>, showing selected atom labeling. Hydrogens on carbon have been omitted.

<sup>†</sup> Electronic supplementary information (ESI) available: DFT geometry optimized structures of isomeric RuCl(CO)(PMe<sub>3</sub>)<sub>2</sub>HSO<sub>2</sub>. See <http://www.rsc.org/suppdata/nj/b2/b212025a/>

The structure of  $\text{RuHCl}(\text{CO})(\text{SO}_2)(\text{P}^i\text{Pr}_3)_2$  is octahedral, with  $\eta^1$ - $\text{SO}_2$  bound trans to hydride. Sulfur is coplanar with its three attached groups, consistent with  $\text{SO}_2$  acting as a Lewis base towards Ru (binding mode A). The  $\text{SO}_2$  ligand is oriented perpendicularly to the P–Ru–P plane, thus assuming the position with the least steric repulsion from the bulky phosphines, as well as minimizing the competition between  $\pi^*$  of  $\text{SO}_2$  and CO for  $d_\pi$  electrons of the metal. The structure<sup>6</sup> of  $\text{OsHCl}(\text{SO}_2)(\text{CO})(\text{PCy}_3)_2$  (not crystallographically isomorphous) is remarkably similar to that of  $\text{RuHCl}(\text{SO}_2)(\text{CO})(\text{P}^i\text{Pr}_3)_2$ , even regarding the eclipsing of the  $\text{SO}_2$  plane with the Cl–M–CO vector. Ru–P bond distances (2.372 Å) are similar to the distances (2.379 Å) observed for the five-coordinate precursor  $\text{RuHCl}(\text{CO})(\text{PPr}_3)_2$ <sup>13</sup>, while the Ru–Cl bond is very slightly elongated (2.438 *vs.* 2.422 Å). One of the most interesting structural features of this compound is the unusually long Ru–S bond length (2.285 Å), which is about 0.20 Å longer than the Ru–S bond in  $[\text{Ru}(\text{NH}_3)_4(\text{SO}_2)\text{Cl}]\text{Cl}$ <sup>11</sup> and is the consequence of the strong trans influence of the hydride ligand. This bond is longer (2.239 Å) than the Os–S bond in  $\text{OsHCl}(\text{CO})(\text{SO}_2)(\text{PCy}_3)_2$ <sup>6</sup>, apparently because it is weakened due to the poorer  $\pi$ -donor ability of Ru in comparison to Os.

### DFT evaluation of isomeric structures

**Intact  $\text{SO}_2$  as a ligand.** DFT energy minimization of  $\text{RuHCl}(\text{SO}_2)(\text{CO})(\text{PMe}_3)_2$  as a model of the  $\text{P}^i\text{Pr}_3$  analog yields [Fig. 2(a)] one structure in which  $\text{SO}_2$  bonds  $\eta^1$  and trans to hydride, consistent with the experimental structure (Table 1). The geometry is planar at sulfur and the plane of the  $\text{SO}_2$  group nearly eclipses the RuCl bond; the dihedral angle Cl–Ru–S–O averages 25°. The energy when this angle is 0° is insignificantly (1 kcal mol<sup>−1</sup>) higher. The same is true for the alternative conformer calculated with eclipsed Ru–P and S–O bonds. Bond lengths and angles within the  $\text{RuHCl}(\text{CO})(\text{PMe}_3)_2$  substructure are in satisfactory agreement with experiment (Table 1), as are the parameters within the  $\text{SO}_2$  unit and the Ru–S distance.

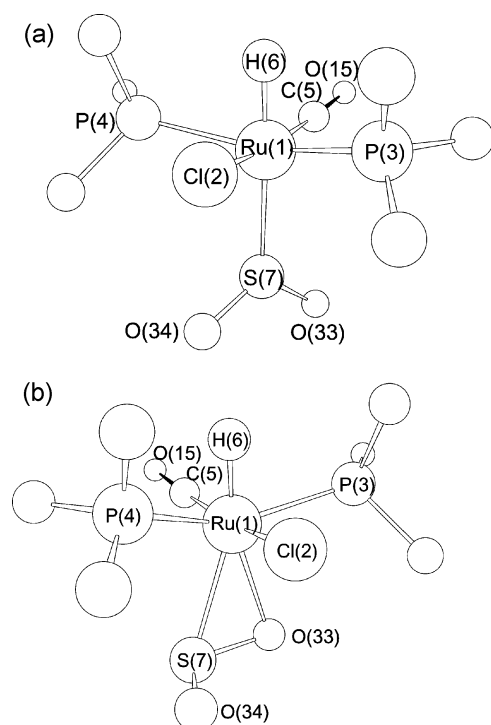


**Fig. 2** DFT optimized geometries of (a)  $\text{RuHCl}(\text{CO})(\eta^1\text{-SO}_2)(\text{PMe}_3)_2$  and (b)  $\text{RuHCl}(\text{CO})(\eta^2\text{-SO}_2)(\text{PMe}_3)_2$ . Methyl hydrogens have been omitted. Selected structural parameters for (b): Ru–Cl, 2.474; Ru–S, 2.570; S7–O33, 1.556; S7–O34, 1.498 Å.

**Table 1** Selected bond distances (Å) and angles (°) for  $\text{RuHCl}(\text{SO}_2)(\text{CO})(\text{P}^i\text{Pr}_3)_2$

	X-ray	DFT (PME <sub>3</sub> )
Ru(1)–C(15)	1.843(5)	1.878
Ru(1)–S(12)	2.285(3)	2.333
Ru(1)–P(2)	2.4075(8)	2.405
Ru(1)–Cl(14)	2.4375(16)	2.476
S(12)–O(13)	1.4358(17)	1.492
C(15)–O(16)	1.106(5)	1.165
Ru–H(22)	1.54	1.62
C(15)–Ru(1)–S(12)	92.73(19)	93.8
C(15)–Ru(1)–P(2)′	89.14(14)	96.1
C(15)–Ru(1)–P(2)	89.91(14)	93.1
S(12)–Ru(1)–P(2)	99.95(7)	98.1
P(2)′–Ru(1)–P(2)	160.10(13)	160.8
C(15)–Ru(1)–Cl(14)	172.7(2)	171.5
S(12)–Ru(1)–Cl(14)	94.53(7)	94.6
P(2)′–Ru(1)–Cl(14)	87.98(5)	84.1
P(2)–Ru(1)–Cl(14)	90.45(5)	84.4
O(13)–S(12)–O(13)′	114.96(14)	116.0
O(13)–S(12)–Ru(1)	122.52(7)	121.8

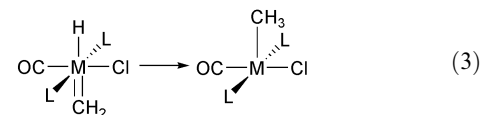
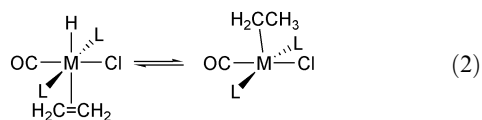
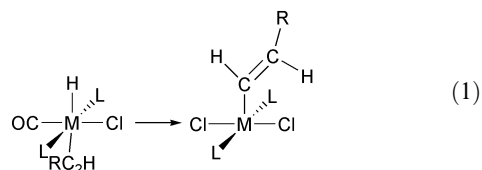
Another minimum was found [Fig. 2(b)] with  $\text{SO}_2$  bound  $\eta^2$ , through S and one O. This structure exhibits the feature observed in other  $\eta^2$ - $\text{SO}_2$  complexes,<sup>1</sup> which is a pyramidal sulfur; the  $\angle$ OSO of coordinated  $\text{SO}_2$  is bent, but not directly away from the metal. Instead, the oxygen not bound to the metal bends in a fashion consistent with one  $\text{SO}_2$   $\pi$  bond interacting with the metal: donation from  $(\pi_{\text{SO}})^2$  to Ru together with back-bonding from Ru to  $\pi_{\text{SO}}^*$ . This direction of bending is a reflection of the orthogonality of the two  $p_\pi$  orbitals on sulfur and thus the orthogonality of the two SO  $\pi$  bonds. The net result is that the SO bond bound to Ru is longer (by 0.06 Å) than the pendant SO bond. Further symptomatic of this back-donation is that  $\angle$ P–Ru–P is smaller (by 8°) in the  $\eta^2$ - $\text{SO}_2$  structure than in the  $\eta^1$ - $\text{SO}_2$  structure, an effect that rehybridizes one occupied  $d_\pi$  metal orbital for better<sup>14</sup> back-donation to  $\pi_{\text{SO}}^*$ . Note that the rotational conformation of the Ru-coordinated SO bond is the one that aligns it with this rehybridized  $d_\pi$  orbital in the P–Ru–P plane, for good back-bonding *and* to avoid  $\pi$  competition between  $\eta^2$ - $\text{SO}_2$  and the CO ligand. At the same time, another minimum was found with eclipsed Ru–Cl and S–O bonds, 0.6 kcal mol<sup>−1</sup> less stable; since this is comparable to thermal energy at 20 °C, this is properly called a second conformer. No stationary point was found for an eclipsed C–Ru–S–O conformation.

A search was made for an  $\eta^1$ - $\text{SO}_2$  isomer with a *pyramidal* sulfur (structure C); this is a bonding form in which the  $\text{SO}_2$  is a Lewis acid, but where the Ru → S bond would be primarily of sigma symmetry. No minimum was located, beginning with structures with pyramidal S and one oxygen eclipsing (1) the Ru–CO, (2) the Ru–Cl and (3) the Ru–P vector. In every case, the geometry optimized to a planar sulfur ( $\eta^1$ ) or to the  $\eta^2$ - $\text{SO}_2$  structure. This absence of a stable  $\eta^1$  structure with pyramidal S is consistent with the fact that a  $\sigma$  bonding orbital directed trans to the hydride in  $\text{RuHCl}(\text{CO})\text{L}_2$  is the LUMO, and thus lacks the electrons to *donate* to S.  $\text{RuHCl}(\text{CO})\text{L}_2$  is primarily a Lewis *acid*, not a base.

The  $\Delta G^\circ_{298}$  for binding  $\text{SO}_2$  to  $\text{RuHCl}(\text{CO})(\text{PMe}_3)_2$  is calculated to be −3.7 kcal mol<sup>−1</sup> for  $\eta^1$ -planar binding and −2.8 kcal mol<sup>−1</sup> for  $\eta^2$  binding. The free energy is small in part due to an unfavorable entropy, but these two binding energies are remarkably similar. The bulkier  $\text{P}^i\text{Pr}_3$  will further bias the isomer preference towards  $\eta^1$  binding (the rotational conformation of the  $\eta^2$ - $\text{SO}_2$  interferes especially with one phosphine).

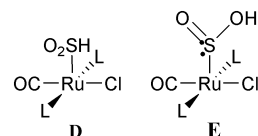
**Insertion of  $\text{SO}_2$  into Ru–H.**  $\text{MHCl}(\text{CO})\text{L}_2$  complexes (M = Ru, Os) have been shown<sup>15</sup> to bind terminal alkynes

trans to hydride in a kinetic product, and then insert to give vinyl complexes [eqn. (1)]. Ethylene binds more weakly and only incompletely inserts to form an ethyl product [eqn. (2)], which is reversed under vacuum.<sup>16</sup> Finally, methylene binds trans to hydride,<sup>17</sup> but, in a thermodynamically highly favorable reaction<sup>18</sup> ( $\Delta E = -25.7 \text{ kcal mol}^{-1}$ ), inserts to form a methyl complex [eqn. (3)]. It is therefore of interest to compare these results to  $\text{SO}_2$  insertion, since the  $\text{SO}_2$  results cited in the introduction here lack a hydride ligand.<sup>19–21</sup>



Two possible insertion products, **D** and **E**, were therefore evaluated. Each (Fig. 3) was found to be an energy minimum. The  $\text{Ru}(\text{CO})\text{Cl}(\text{PMe}_3)_2$  substructures in Fig. 3 have distances and angles similar to those of  $\text{RuHCl}(\text{CO})(\text{PMe}_3)_2$ , and the insertion products are square pyramidal. The  $\text{Ru}-\text{S}(\text{H})\text{O}_2$  complex lies  $8.2 \text{ kcal mol}^{-1}$  ( $\Delta G^\circ_{298}$ ) above  $\text{RuHCl}(\eta^1\text{-SO}_2)(\text{CO})$ -

$(\text{PMe}_3)_2$ , so this reduction of  $\text{SO}_2$  is unfavorable. In contrast, the  $\text{Ru}-\text{SO}(\text{H})$  complex lies  $7.4 \text{ kcal mol}^{-1}$  ( $\Delta G^\circ_{298}$ ) below  $\text{RuHCl}(\eta^1\text{-SO}_2)(\text{CO})(\text{PMe}_3)_2$ . However, there is a short and thus strong hydrogen bond between the OH proton and the Cl on Ru ( $\text{Cl2-H34} = 2.245 \text{ \AA}$ ,  $\angle \text{Cl2-H34-O33} = 160.4^\circ$ ). Since a hydrogen bond is worth at least  $5 \text{ kcal mol}^{-1}$  (and is probably higher for OH on  $\text{S}^{\text{IV}}$ ), most of the  $7.4 \text{ kcal mol}^{-1}$  stability of this isomer is due to hydrogen bonding, and not to general stability of the new functionality formed,  $\text{S}(\text{O})\text{OH}$ .



In sum, none of these insertion products is strongly preferred over  $\text{RuHCl}(\eta^1\text{-SO}_2)(\text{CO})\text{L}_2$ . Experimentally, heating  $\text{RuHCl}(\eta^1\text{-SO}_2)(\text{CO})\text{L}_2$  at  $55^\circ\text{C}$  for 24 h in  $\text{C}_6\text{D}_6$  leaves the molecule unchanged.

## Experimental

### General procedures

All manipulations were carried out using standard Schlenk and glovebox techniques under prepurified argon. Solvents were distilled from drying agents, stored in bulbs with Teflon valves and subjected to three freeze-pump-thaw cycles prior to use.  $\text{SO}_2$  was used as received from Matheson. NMR spectra were recorded on Varian XL 400 MHz instrument with chemical shifts in ppm referenced to residual solvent peaks ( $^1\text{H}$ ) or external  $\text{H}_3\text{PO}_4$  ( $^{31}\text{P}$ ). Infrared spectra were recorded (in Nujol or in an NaCl cavity cell, 0.1 mm path length) on a Nicolet 510 FT-IR spectrometer to a precision of  $0.3 \text{ cm}^{-1}$ .  $\text{RuHCl}(\text{CO})-(\text{P}^i\text{Pr}_3)_2$ <sup>22</sup> and  $\text{OsHCl}(\text{CO})(\text{P}^i\text{Pr}_3)_2$ <sup>19</sup> were prepared using previously published procedures.

### Solid-gas reactions

All solid-gas reactions were carried out in 100 mL Schlenk flasks under 1 atm of gaseous reagent (unless specified otherwise) at room temperature. After the given time, gaseous reagents were removed under vacuum and the composition of products was analyzed by solid-state IR and solution NMR.

**Reaction of  $\text{RuHCl}(\text{CO})(\text{P}^i\text{Pr}_3)_2$  with  $\text{SO}_2$ .** After 12 h of exposure to 1 atm  $\text{SO}_2$  for the solid-gas reaction, or immediately in  $\text{C}_6\text{D}_6$  solution, the reaction mixture turns pale-yellow and the formation of  $\text{RuHCl}(\text{CO})(\text{SO}_2)(\text{P}^i\text{Pr}_3)_2$  is detected by  $^1\text{H}$  and  $^{31}\text{P}$  NMR spectroscopy.  $^1\text{H}$  NMR (400 MHz,  $\text{C}_6\text{D}_6$ ,  $20^\circ\text{C}$ ) ppm:  $-6.57$  (t,  $J_{\text{HH}} = 19 \text{ Hz}$ ,  $\text{RuH}$ ),  $1.37$  (m,  $\text{PCCCH}_3$ ),  $2.69$  (m,  $\text{PCH}$ ).  $^{31}\text{P}\{^1\text{H}\}$  NMR (161.5 MHz,  $\text{C}_6\text{D}_6$ ,  $20^\circ\text{C}$ ) ppm:  $61.4$ (s). IR ( $\text{cm}^{-1}$ ):  $1110$  (sym  $\text{SO}_2$ ),  $1288$  (asym  $\text{SO}_2$ ),  $1965$  (CO),  $2037$  (Ru-H), all in Nujol;  $1113$ ,  $1292$ ,  $1966$  in  $\text{C}_6\text{H}_6$ .

**Reaction of  $\text{OsHCl}(\text{CO})(\text{P}^i\text{Pr}_3)_2$  with  $\text{SO}_2$ .** After 12 h of exposure to 1 atm  $\text{SO}_2$  for the solid-gas reaction, or immediately in  $\text{C}_6\text{D}_6$  solution, the reaction mixture turns pale-yellow and the formation of  $\text{RuHCl}(\text{CO})(\text{SO}_2)(\text{P}^i\text{Pr}_3)_2$  is detected by  $^1\text{H}$  and  $^{31}\text{P}$  NMR spectroscopy.  $^1\text{H}$  NMR (400 MHz,  $\text{C}_6\text{D}_6$ ,  $20^\circ\text{C}$ ) ppm:  $-7.03$  (t,  $J_{\text{HH}} = 22 \text{ Hz}$ ,  $\text{RuH}$ ),  $1.13$  (m,  $\text{PCCCH}_3$ ),  $2.53$  (m,  $\text{PCH}$ ).  $^{31}\text{P}\{^1\text{H}\}$  NMR (121.4 MHz,  $\text{C}_6\text{D}_6$ ,  $20^\circ\text{C}$ ) ppm:  $29.0$ (s). IR ( $\text{cm}^{-1}$ ):  $1114$  (sym  $\text{SO}_2$ ),  $1288$  (asym  $\text{SO}_2$ ),  $1955$  (CO), all in  $\text{C}_6\text{D}_6$ .

### Crystal structure determination of $\text{RuHCl}(\text{CO})(\text{SO}_2)(\text{P}^i\text{Pr}_3)_2$

The sample consisted of small orange crystals growing together as a layered "clump". Several crystals were examined in the course of the study. The first sample revealed a monoclinic

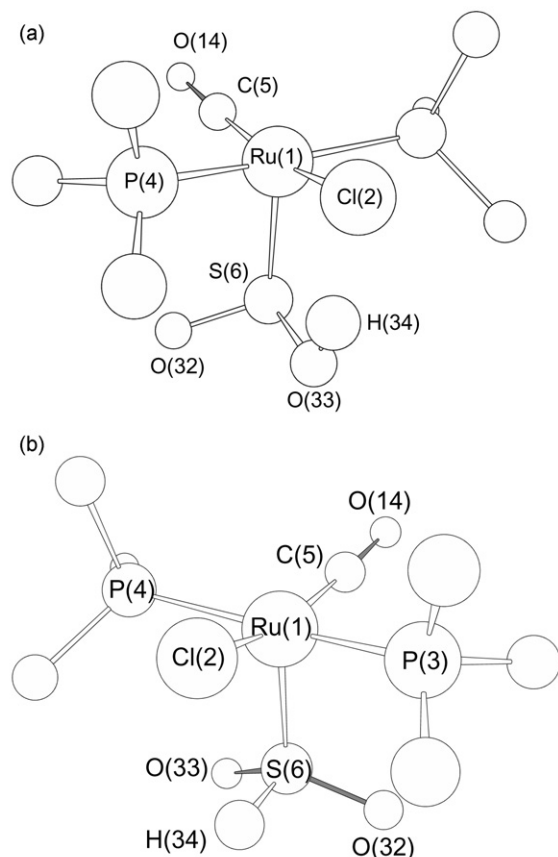


**Fig. 3** DFT optimized geometries of (a)  $\text{Ru}[\text{SO}(\text{OH})]\text{Cl}(\text{CO})(\text{PMe}_3)_2$  and (b)  $\text{Ru}[\text{S}(\text{O})_2\text{H}]\text{Cl}(\text{CO})(\text{PMe}_3)_2$ . Selected structural parameters for (a):  $\text{Ru}-\text{Cl}$ ,  $2.468$ ;  $\text{Ru}-\text{S}$ ,  $2.322$ ;  $\text{S6}-\text{O32}$ ,  $1.514$ ;  $\text{S6}-\text{O33}$ ,  $1.713$ ;  $\text{O33}-\text{H34}$ ,  $0.990 \text{ \AA}$  and for (b)  $\text{Ru}-\text{Cl}$ ,  $2.426$ ;  $\text{Ru}-\text{S}$ ,  $2.267$ ;  $\text{S}-\text{O32}$ ,  $1.502$ ;  $\text{S}-\text{O33}$ ,  $1.502$ ;  $\text{S}-\text{H}$   $1.401 \text{ \AA}$ .



**Table 2** Crystal data for RuHCl(SO<sub>2</sub>)(CO)(P<sup>i</sup>Pr<sub>3</sub>)<sub>2</sub>

Empirical formula	C <sub>19</sub> H <sub>43</sub> ClO <sub>3</sub> P <sub>2</sub> RuS
Formula weight	550.05
Crystal system	Monoclinic
Space group	C2/c
T/K	112(2)
a/Å	21.693(4)
b/Å	8.7000(17)
c/Å	15.410(3)
α/°	90
β/°	119.20(3)
γ/°	90
Z	4
U/Å <sup>3</sup>	2538.7(9)
λ/Å	0.71073
μ/mm <sup>-1</sup>	0.947
Total reflections	3833
Unique reflections	3686
Obsd reflections [ <i>F</i> > 4σ( <i>F</i> )]	3039
<i>R</i> for averaging	0.036
<i>R</i> ( <i>F</i> ) (observed data)	0.0234
<i>R</i> <sub>w</sub> ( <i>F</i> <sup>2</sup> ) (refinement data)	0.0524

space group with a disordered molecule lying at a center of inversion. A second crystal revealed a C-centered monoclinic cell. Several other crystals were examined, two of these in the original space group, and three of these in the C-centered space group. This report describes the latter (see Table 2 for selected data). A typical plate was cleaved from the mass and a nearly equidimensional fragment obtained. The sample was then affixed to a glass fiber using silicone grease and transferred to the Bruker SMART6000 CCD system where it was cooled to −161 °C using a gas-flow cooling system of local design. The data were collected using 3 s frames with an omega scan of 0.30°. Data were corrected for Lorentz and polarization effects and equivalent reflections averaged using the Bruker SAINT software as well as utility programs from the XTEL library. The structure was solved using SHELXTL and Fourier techniques. The molecule lies on a two-fold axis with two disorder problems. The carbonyl and chlorine ligands are disordered with 50% occupancy. After this rotational disorder was properly modeled, it was found that there was a residual peak of several electrons lying on the two-fold axis near the Ru atom. When this peak was refined as a partial occupancy Ru atom the refinement converged with the alternate site being at 5.7% occupancy. There is no evidence of an alternate chlorine position for this second Ru; the occupancy of the S and O atoms converged to 83.8% and 82.4%. It is thus apparent that there is ~6% RuHCl(CO)(P<sup>i</sup>Pr<sub>3</sub>)<sub>2</sub> impurity co-crystallized with the SO<sub>2</sub> adduct. After the compositional disorder was properly modeled it was possible to locate and refine all hydrogen atoms. In a difference Fourier map, a peak was found that is reasonable for the hydride atom, and it was included in the final cycles. It should be emphasized that while the hydride is in a logical position, the disorder present makes its position suspect. The final difference Fourier map was essentially featureless, the largest peak being 0.81 e Å<sup>-3</sup>.

CCDC reference number 200122. See <http://www.rsc.org/suppdata/nj/b2/b212025a/> for crystallographic files in CIF or other electronic format.

### DFT calculations

Theoretical calculations in this work have been performed using the density functional theory (DFT) method;<sup>23</sup> specifically the generalized gradient approximation (GGA) for the exchange-correlation functional by Perdew, Burke and Ernzerhof (PBE)<sup>24</sup> was employed, implemented in an original

program package “Priroda”.<sup>25</sup> In PBE calculations, relativistic Stevens–Basch–Krauss (SBK) effective core potentials (ECP)<sup>26</sup> optimized for DFT calculations have been used. The basis set was 311-split for main group elements with one additional polarization p function for hydrogen, and with two additional polarization d functions for elements of higher periods. Full geometry optimization has been performed without constraints on symmetry using analytical gradients and followed by analytical calculation of the second derivatives of energy with respect to coordinate in order to characterize the nature of the resulting stationary points (minima or saddle points) found on the potential energy surface. For all species under investigation, frequency analysis has been carried out. All minima have been checked for the absence of imaginary frequencies. Zero point vibrational energies and thermodynamic functions were calculated in the harmonic approximation.

### Acknowledgements

This work was supported by the Department of Energy.

### References

- 1 R. R. Ryan, G. J. Kubas, D. C. Moody and P. G. Eller, *Struct. Bonding (Berlin)*, 1981, **46**, 47.
- 2 J. Shen, G. J. Kubas and A. L. Rheingold, *Inorg. Chim. Acta*, 1995, **240**, 99.
- 3 G. J. Kubas, G. D. Jarvinen and R. R. Ryan, *J. Am. Chem. Soc.*, 1983, **105**, 1883.
- 4 G. J. Kubas, R. R. Ryan and V. McCarty, *Inorg. Chem.*, 1980, **19**, 3003.
- 5 G. J. Kubas, *Inorg. Chem.*, 1979, **18**, 182.
- 6 R. R. Ryan and G. J. Kubas, *Inorg. Chem.*, 1978, **17**, 637.
- 7 D. A. Johnson and V. C. Dew, *Inorg. Chem.*, 1979, **18**, 3273.
- 8 A. Y. Kovalevsky, K. A. Bagley and P. Coppens, *J. Am. Chem. Soc.*, 2002, **124**, 9241.
- 9 J. K. Shen, F. Basolo and G. J. Kubas, *J. Organomet. Chem.*, 1995, **488**, C1.
- 10 J. P. Collman, L. S. Hegedus, J. R. Norton and R. G. Finke, *Principles and Applications of Organotransition Metal Chemistry*, University Science Books, Mill Valley, CA, 1987.
- 11 L. H. Vogt, Jr., J. L. Katz and S. E. Wiberly, *Inorg. Chem.*, 1965, **4**, 1157.
- 12 F. G. Moers, R. W. M. Ten Hoedt and J. P. Langhout, *Inorg. Chem.*, 1973, **12**, 2196.
- 13 D. Huang, W. E. Streib, J. C. Bollinger, K. G. Caulton, R. F. Winter and T. Scheiring, *J. Am. Chem. Soc.*, 1999, **121**, 8087.
- 14 D. V. Yandulov, D. Huang, J. C. Huffman and K. G. Caulton, *Inorg. Chem.*, 2000, **39**, 1919.
- 15 A. V. Marchenko, H. Gerard, O. Eisenstein and K. G. Caulton, *New J. Chem.*, 2001, **25**, 1244.
- 16 A. V. Marchenko, H. Gerard, O. Eisenstein and K. G. Caulton, *New J. Chem.*, 2001, **25**, 1382.
- 17 D. Huang, G. J. Spivak and K. G. Caulton, *New J. Chem.*, 1998, **22**, 1023.
- 18 H. Gerard, E. Clot and O. Eisenstein, *New J. Chem.*, 1999, **23**, 495.
- 19 G. J. Kubas, H. J. Wasserman and R. R. Ryan, *Organometallics*, 1985, **4**, 2012.
- 20 S. L. Randall, C. A. Miller, T. S. Janik, M. R. Churchill and J. D. Atwood, *Organometallics*, 1994, **13**, 141.
- 21 The subject has been discussed on pages 185–187 of: G. J. Kubas, *Acc. Chem. Res.*, 1994, **27**, 183.
- 22 M. A. Esteruelas and H. Werner, *J. Organomet. Chem.*, 1986, **303**, 221.
- 23 R. G. Parr and W. Yang, *Density Functional Theory of Atoms and Molecules*, Oxford University Press, Oxford, 1989.
- 24 J. P. Perdew, K. Burke and M. Ernzerhof, *Phys. Rev. Lett.*, 1996, **77**, 3865.
- 25 Y. A. Ustynyuk, L. Y. Ustynyuk, D. N. Laikov and V. V. Lunin, *J. Organomet. Chem.*, 2000, **597**, 182.
- 26 W. J. Stevens, H. Basch and M. Krauss, *J. Chem. Phys.*, 1984, **81**, 6026; W. J. Stevens, H. Basch, M. Krauss and P. Jasien, *Can. J. Chem.*, 1992, **70**, 612; T. R. Cundari and W. J. Stevens, *J. Chem. Phys.*, 1993, **98**, 5555.